

THE PREPARATION AND CHARACTERIZATION OF $W_{18}O_{49}@PEG$ PHOTOTHERMAL AGENT

Y. Q. LIANG^a, X. F. GAO^b, X. J. LI^{b,*}, W. Q. ZHANG^b, J. S. LIAN^a

^aKey Laboratory of Automobile Materials, Ministry of Education, Department of Materials Science and Engineering, Jilin University, Changchun, 130025, China

^bCollege of Materials Science and Engineering, Harbin University of Science and Technology, Harbin, China

Photothermal therapy using traditional conversion agent was limited by the complexity of cancer. It was urgent to find a new efficient and inoffensive photothermal conversion agent. Herein, we synthesized $W_{18}O_{49}$, a non-invasive and efficient photothermal conversion agent for photothermal therapy application. This work revealed that the morphology of $W_{18}O_{49}$ was changed for photothermal therapy by poly ethylene glycol (PEG) modification. Meanwhile, with 808 nm irradiation, $W_{18}O_{49}@PEG$ nanoparticles could convert laser energy into hyperthermia, which could further induce cancer cells ablation.

(Received February 23, 2020; Accepted May 22, 2020)

Keywords: $W_{18}O_{49}@PEG$, Morphology, Near-infrared, Photothermal agent

1. Introduction

Cancer has seriously threatened the health of human beings [1], gradually promoting various clinical treatments. Comparing with traditional therapeutic treatments, photothermal therapy brings the photothermal conversion agents to an excited state where it then releases vibrational energy to induce the targeted cancer cells ablation [2], which is an efficient and inoffensive treatment for thermal ablation of tumor cells. With the rapid development of nanomaterials that enhanced permeability and retention effects (EPR) [3] as cancer therapeutic agents themselves, it becomes possible to find an accurate and sensitive photothermal conversion agent.

Carbon-based nanomaterial (e.g. nanostructured graphene [4], carbon dots [5]), gold nanostructures (e.g. Au nanorods or nanowires) [6-7], metal oxide (e.g. $W_{18}O_{49}$ [8]), metal sulfide (e.g. CuS) [9] and NIR-absorbing organic dyes [10] could absorb NIR light then generate heat to ablation tumor cells. $W_{18}O_{49}$ nanoparticle was reported for photothermal therapy due to the localized surface plasmon resonance [11] and W element ($Z>50$) could be used for computerized tomography imaging (CT) [12]. Furthermore, $W_{18}O_{49}$ nanocrystals have three valence states (such

* Corresponding author: lixuejiao@hrbust.edu.cn.

as W^{6+} , W^{5+} and W^{4+}) because of their special structural defect, which cause strong absorption in the near infrared region, as shown in Fig. 1(a). However, the uncontrollable morphology and weak biocompatibility limited the application of $W_{18}O_{49}$ *in vivo*. PEG is a polymer of linear structure which could interact with metal ions then grow into special shape along the polymer chain. According to unique molecular structure, the good effects of PEG could make the whole nanoparticles for applying to clinical treatments [13]. Thus, $W_{18}O_{49}@PEG$ nanoparticle is potential to be a photothermal conversion agent under near-infrared light irradiation *in vivo*.

The NIR region (700-1100 nm), which has deep light penetration and low light absorption, is known as the transparent window of the biological window [11]. In early study, PEGylated $W_{18}O_{49}$ nanowires as shown in Fig. 1(b) were synthesized for *in vivo* tumor therapy by 980 nm light activated irradiation [14]. However, 980 nm near-infrared light would cause unfavorable heating effect on the normal tissues [15]. Normal tissue does not produce excessive heat when illuminated at 808 nm [16]. In our work, $W_{18}O_{49}$ was modified with PEG to construct $W_{18}O_{49}@PEG$ nanoparticles. With the ideal morphology, nanoparticles were still able to trigger thermal energy in 808 nm irradiation for ablation of cancer cells.

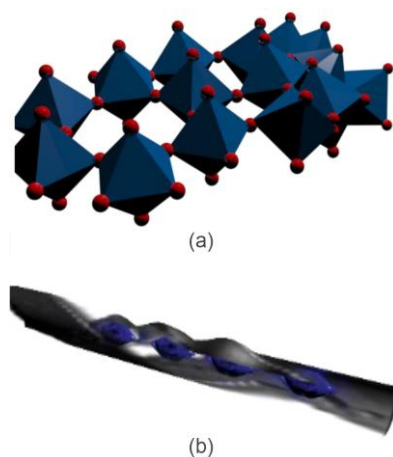


Fig.1. (a) The molecular structure of $W_{18}O_{49}$ and (b) the predicted structure of $W_{18}O_{49}@PEG$.

2. Experimental

2.1. Materials

Tungsten (VI) chloride (WCl_6 , AR) were purchased from Aladdin Reagent Co.Ltd., Polyethylene glycol ($HO-(CH_2CH_2O)-nH$) were obtained from Tianjin kangfu Institute of fine chemicals. 1-propanol were obtained from Tianjing Kermel Chemical Reagent Co.Ltd.. All chemicals were analytical reagents and could be used directly without further purification.

(Preparation)

2.2. Synthesis of $W_{18}O_{49}$ nanoparticles

WCl_6 (0.2g) was dissolved in n-propanol (40 mL) to make a transparent yellow solution under magnetically stirring. The solution was then transferred into a Teflon-lined stainless steel autoclave and sealed, maintained at 180 °C for 24 h. Finally, the product was washed with deionized water and ethanol each for three times.

2.3. Synthesis of $W_{18}O_{49}$ @PEG nanoparticles

WCl_6 (0.2 g) was dissolved in n-propanol (14 mL) and PEG (26 mL), the solution was then forming a transparent yellow solution after magnetically stirring until the solid powder was completely dissolved in the oily solution. After transferring the solution into a Teflon-lined stainless steel autoclave and sealed, the solution should be maintained at $180\text{ }^{\circ}\text{C}$ for 24 h. Finally, the product was washed with deionized water and ethanol each for three times.

2.4. Characterization

The phase of the products was identified by X-ray diffraction (XRD, PANalytical X'Pert PRO MPD, Holland) with Cu-K α radiation ($\lambda = 0.154056\text{ nm}$). Morphological features of the products were observed using transmission electron microscopy (TEM, JEM2100, Japan) and scanning electron microscope (SEM, FEI Sirion 200, FEI). The fourier transform infrared (FT-IR, CZ304, Japan) was used to detect different functional groups. The products were excited by 808 nm laser provided by NINGBO LASEVER INC.

3. Result and discussion

To determine the phase purity of the products, XRD measurements for the synthesized products were conducted. Fig. 2 showed the XRD patterns of $W_{18}O_{49}$ and $W_{18}O_{49}$ @PEG. Obviously, there was no difference between $W_{18}O_{49}$ and $W_{18}O_{49}$ @PEG, which was definitely matching with the PDF card 71-2450. After modification by PEG, the peak of $W_{18}O_{49}$ @PEG was smoother. The intensity of the main peak that located at 23° was reduced.

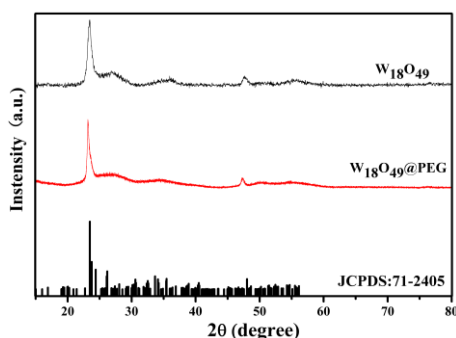


Fig. 2. XRD patterns of $W_{18}O_{49}$ and $W_{18}O_{49}$ @PEG.

Fig. 3 shows the covalent bond information for $W_{18}O_{49}$ and $W_{18}O_{49}$ @PEG. According to the spectra, the band at $1564\text{--}1582\text{ cm}^{-1}$ was attributed to C=C stretches. The presence of the intense absorption peak at $3411\text{--}3698\text{ cm}^{-1}$ indicated the stretching vibration of O-H. $W_{18}O_{49}$ @PEG has C-O stretching vibration at 1094 cm^{-1} , indicating that PEG as a modification effect on $W_{18}O_{49}$.

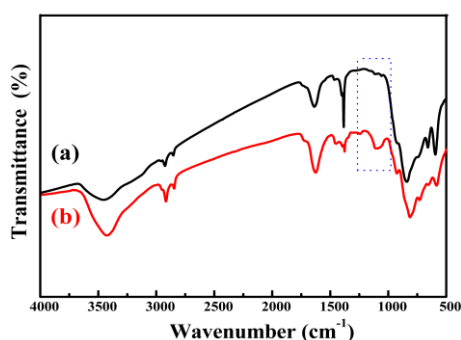


Fig. 3. FT-IR spectra of $W_{18}O_{49}$ (a) and (b) $W_{18}O_{49}@PEG$

Like crystal structure, another essential property of the nanostructure is its morphology. Transmission electron microscope (TEM) and scanning electron microscope (SEM) were used for morphology observation. TEM images of the $W_{18}O_{49}$ and $W_{18}O_{49}@PEG$ were shown in Fig. 4(a) and (b). In Fig. 4(a), the size of the prepared $W_{18}O_{49}$ were about 100 nm, and the HRTEM (High Resolution Transmission Electron Microscope) image indicated the interplanar distances between adjacent lattice planes was 0.378 nm, which was well coincident with the (010) lattice of $W_{18}O_{49}$.

$W_{18}O_{49}@PEG$ was shown in Fig. 4(b), the morphology of the nanoparticles changed from fusiform to linear, and the width of each nanowire was about 5 nm. After ultrasonic probe processing, the length of $W_{18}O_{49}@PEG$ nanowires was shorter and their dispersion was improved significantly. SEM images of $W_{18}O_{49}$ and $W_{18}O_{49}@PEG$ were shown in Fig. 4(c) and (d). Uniform and stable $W_{18}O_{49}$ nanoparticles were performed in Fig. 4(c). Meanwhile, as depicted in Fig. 4(d), folded spherical particles were shown after modifying PEG. The adjustment of the morphology was attributed to the modification by PEG.

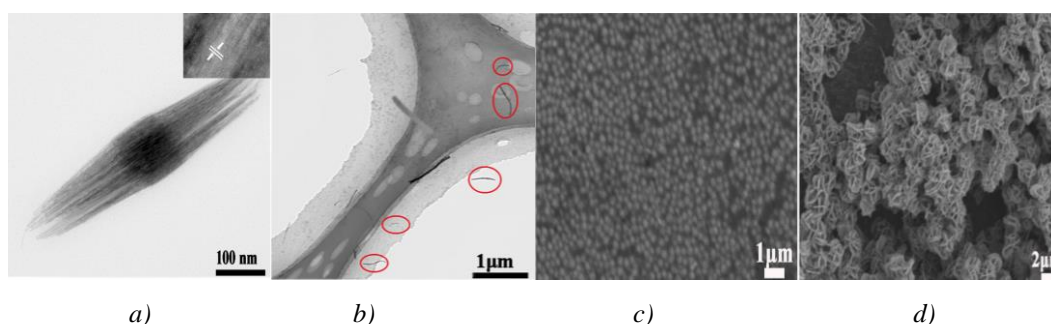


Fig. 4. TEM and SEM images of $W_{18}O_{49}$ and $W_{18}O_{49}@PEG$. (a) TEM image of $W_{18}O_{49}$ (b) TEM image of $W_{18}O_{49}@PEG$ after ultrasonic probe (c) SEM image of $W_{18}O_{49}$ (d) SEM image of $W_{18}O_{49}@PEG$.

The 808 nm irradiation induced heat generation of $W_{18}O_{49}$ and $W_{18}O_{49}@PEG$ was shown in Fig. 5. Under 808 nm irradiation, the temperature of $W_{18}O_{49}$ and $W_{18}O_{49}@PEG$ that were dissolved in deionized water increased distinctly with time. The $W_{18}O_{49}@PEG$ nanoparticles could reach the temperature of 44 °C in 10 min, which is above the apoptosis inducing

temperature of cancer cells (39 °C) and only about 3 °C higher than $W_{18}O_{49}$. The temperature increase indicated that $W_{18}O_{49}@PEG$ nanowires could convert the laser energy into hyperthermia with 808 nm irradiation.

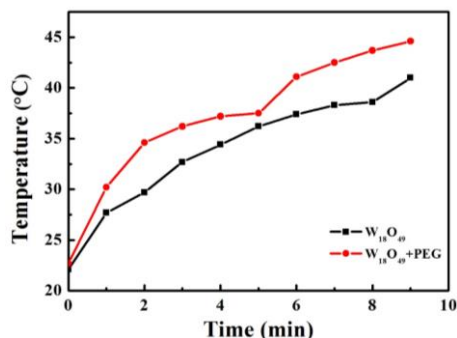


Fig. 5. 808 nm induced heat generation of $W_{18}O_{49}$ and $W_{18}O_{49}@PEG$.

4. Conclusions

In summary, we used the solvothermal method for preparing $W_{18}O_{49}$ and $W_{18}O_{49}@PEG$ which show different morphologies. After PEG modification, the width of nanoparticles was decreased to 5 nm. By controlling the time of ultrasonic processing, the nanoparticle length can be shortened. The reduction of nanoparticle size would increase EPR, which is potential to increase efficacy and reduce side effects of normal tissue. In addition, $W_{18}O_{49}@PEG$ nanoparticles exhibit stronger light absorption ability in 808 nm irradiation than $W_{18}O_{49}$. The temperature of $W_{18}O_{49}@PEG$ after 10 min irradiation was about 8% higher than $W_{18}O_{49}$. Therefore, comparing to $W_{18}O_{49}$, $W_{18}O_{49}@PEG$ nanoparticle is a better candidate of the photothermal conversion agent for cancer treatment.

Acknowledgements

This project was supported by China Postdoctoral Science Foundation (No.2019M651940), Natural Science Foundation of Heilongjiang Province (No. QC2017056) and University Nursing Program for Young Scholars with Creative Talents in Heilongjiang Province (No. 2018204).

References

- [1] A. S. Cleary, T. L. Leonard, S. A. Gestl, E. J. Gunther, *Nature* **508**, 113 (2014).
- [2] W. B. Fan, P. Yung, P. Huang, X. Y. Chen, *Chem. Rev.* **117**, 13566 (2017).
- [3] K. Sano, T. Nakajima, P. L. Choyke, H. Kobayashi, *ACS Nano* **7**, 717 (2013).
- [4] L. Cheng, K. Yang, Y. Li, J. Chen, C. Wang, M. W. Shao, S-T. Lee, Z. Liu, *Angew. Chem. Int. Ed.* **50**, 7385 (2011).
- [5] K. A. Willets, R. P. Van Duyne, *Annu. Rev. Phys. Chem.* **58**, 267 (2007).

- [6] Y. K. Kim, H. K. Na, S. Kim, H. Jang, S. J. Chang, D. H. Min, *Small* **11**, 2527 (2015).
- [7] N. M. Jassim, Z. T. Khodair, M. H. Diwan, M. H. Altimimi, *J. Ovonic Res.* **15**, 221 (2019).
- [8] L. Cheng, C. Wang, L. Feng, K. Yang, Z. Liu, *Chem. Rev.* **114**, 10869 (2014).
- [9] F. Lu, J. Wang, L. Yang, J. J. Zhu, *Chem. Commun.* **51**, 9447 (2015).
- [10] Z. Sun, H. Xie, S. Tang, X-F. Yu, Z. Guo, J. Shao, H. Zhang, H. Huang, H. Wang, P. K. Chu, *Angew. Chem. Int. Ed.* **54**, 11526 (2015).
- [11] P. Huang, Y. Gao, J. Lin, H. Hu, H-S. Liao, X. Yan, Y. Tang, A. Jin, J. Song, G. Niu, G. Zhang, F. Horkay, X. Chen, *ACS Nano* **9**, 9517 (2015).
- [12] Q. Chen, C. Wang, L. Cheng, W. He, Z. Cheng, Z. Liu, *Biomaterials* **35**, 2915 (2014).
- [13] K. Poliraju, V. Raviraj, C Chi-Shiun, K. C. Hwang, *Angew. Chem. Int. Ed.* **125**, 12558 (2013).
- [14] G. Ajithkumar, B. Yoo, D. E. Goral, P. J. Hornsby, A-L. Lin, U. Ladiwala, V. P. Dravid, D. K. Sardara, *J. Mater. Chem. A* **1**, 1561 (2013).
- [15] Q. Zhan, J. Qian, H. Liang, G. Somesfalean, D. Wang, S. He, Z. Zhang, S. Andersson-Engels, *ACS Nano* **5**, 3744 (2011).
- [16] K. Deng, Z. Hou, X. Deng, P. Yang, C. Li, J. Lin, *Adv. Funct. Mater.* **25**, 7280 (2015).